

University of Groningen

Effects of Acetate on Cation Exchange Capacity of a Zn-Containing Montmorillonite

Stathi, P.; Papadas, I. T.; Enotiadis, A.; Gengler, R. Y. N.; Gournis, D.; Rudolf, P.; Deligiannakis, Y.

Published in:
Langmuir

DOI:
[10.1021/la900831q](https://doi.org/10.1021/la900831q)

IMPORTANT NOTE: You are advised to consult the publisher's version (publisher's PDF) if you wish to cite from it. Please check the document version below.

Document Version
Publisher's PDF, also known as Version of record

Publication date:
2009

[Link to publication in University of Groningen/UMCG research database](#)

Citation for published version (APA):

Stathi, P., Papadas, I. T., Enotiadis, A., Gengler, R. Y. N., Gournis, D., Rudolf, P., & Deligiannakis, Y. (2009). Effects of Acetate on Cation Exchange Capacity of a Zn-Containing Montmorillonite: Physicochemical Significance and Metal Uptake. *Langmuir*, 25(12), 6825-6833. <https://doi.org/10.1021/la900831q>

Copyright

Other than for strictly personal use, it is not permitted to download or to forward/distribute the text or part of it without the consent of the author(s) and/or copyright holder(s), unless the work is under an open content license (like Creative Commons).

The publication may also be distributed here under the terms of Article 25fa of the Dutch Copyright Act, indicated by the "Taverne" license. More information can be found on the University of Groningen website: <https://www.rug.nl/library/open-access/self-archiving-pure/taverne-amendment>.

Take-down policy

If you believe that this document breaches copyright please contact us providing details, and we will remove access to the work immediately and investigate your claim.

Downloaded from the University of Groningen/UMCG research database (Pure): <http://www.rug.nl/research/portal>. For technical reasons the number of authors shown on this cover page is limited to 10 maximum.

Effects of Acetate on Cation Exchange Capacity of a Zn-Containing Montmorillonite: Physicochemical Significance and Metal Uptake

P. Stathi,[†] I. T. Papadas,[†] A. Enotiadis,[‡] R. Y. N. Gengler,[§] D. Gournis,[‡] P. Rudolf,[§] and Y. Deligiannakis^{*,†}

[†]Department of Environmental and Natural Resources Management, University of Ioannina, Seferi 2 30100 Agrinio, Greece, [‡]Department of Materials Science & Engineering, University of Ioannina, 45110 Ioannina, Greece, and [§]Zernike Institute for Advanced Materials, University of Groningen, Nijenborgh 4, NL 9747 AG Groningen, The Netherlands

Received November 26, 2008. Revised Manuscript Received April 15, 2009

Fundamental properties such as cation exchange capacity (CEC), permanent charge, pH_{PZC} , and metal uptake of a Zn-containing montmorillonite are modified, in a predictable manner, by a mild chemical treatment using acetate. Acetate treatment allows a controllable increase of the CEC of montmorillonite up to 180 mequiv/100 g. The CEC of the clay is increasing for decreasing Zn content, with a slope of $\Delta[\text{Zn}]/\Delta[\text{CEC}] \approx -2$. X-ray powder diffraction analysis shows that the lamellar structure of the clay remains unaltered by the acetate treatment, while XPS substantiates the removal of Zn. H^+ uptake data show that the intrinsic protonation pK values and concentration of the variable charge sites ($\equiv\text{SOH}$) are not modified by the acetate treatment. In contrast, the concentration of the permanent charge sites ($\equiv\text{X}^-$) increased linearly with Zn removal by acetate, leading to a significant H^+ and Cd^{2+} uptake enhancement. A physical model is suggested where acetate removes Zn ions strongly bound in the clay, and this in turn modulates the permanent charge and the CEC of the clay.

1. Introduction

Clay minerals are among the most important soil constituents. The range of applications of clay minerals is continuously growing due to their unique properties, such as high specific area, fine particle size, swelling, intercalation, and ion exchange. Unmodified and modified clay minerals are widely used as adsorbents¹ or catalyst supports.²

It is well-known that montmorillonite particles carry two kinds of electrical charges^{3–6} which are conveniently discriminated from their pH-dependence:

- A pH-dependent, variable charge, resulting from H^+ adsorption/desorption reactions on surface hydroxyl groups.⁷ Surface hydroxyl groups ($\equiv\text{SOH}$) in aluminosilicate smectites are located at the particle edges, originating from broken or hydrolyzed Al–O and Si–O bonds.⁸ In this context, the pH-dependent charge of the clay is usually assumed to originate from the reactions of the amphoteric surface OH groups which can bear a charge +1 or –1 or zero.³
- A structural, permanent, negative charge ($\equiv\text{X}^-$). In montmorillonites, the latter arises from substitutions in the octahedral alumina sheet, which is

separated from the aqueous solution by a tetrahedral sheet carrying almost no reactive surface groups.⁸ The negative charge resides on the oxygen ions that form the bases of the tetrahedra, which comprise the basal surfaces of the clay layer, and on the apical oxygens which form the internal links between the octahedral and tetrahedral sheets. The basal oxygens are not protonated, except for a very small fraction that are present at the truncated edges of the layers.^{9,10} The structural negative charges ($\equiv\text{X}^-$) induce a net negative electrostatic potential that influences the electrical, sorptive, and coagulative properties of the particles.¹¹ Due to this negative potential, montmorillonite has negative electrophoretic mobilities and very important cation adsorption and cation exchange (CEC) properties. These cation exchange sites influence many important physical properties such as the location of the interlayer cations and the structure of the interlayer cation.¹²

Both permanent and variable charge sites act as binding sites for H^+ , metal ions, or organic molecules. Therefore, a number of studies have been performed using clays for heavy metal adsorption,^{1–7} demonstrating their effectiveness for removal of heavy metals or organic molecules^{13,14} from aqueous solution.

It is well-established that adsorption of ions on clay minerals is controlled by two different mechanisms:⁸ (a) a pH-dependent

*Corresponding author. E-mail: ideligia@cc.uoi.gr.

(1) Kraepiel, A. M. L.; Keller, K.; Morel, F. M. M. *J. Colloid Interface Sci.* **1999**, *210*, 43–54.

(2) Moronta, A.; Ferrer, V.; Quero, J.; Arteaga, G.; Choren, E. *Appl. Catal. A* **2002**, *230*, 127–135.

(3) Kraepiel, A. M. L.; Keller, K.; Morel, F. M. M. *Environ. Sci. Technol.* **1998**, *32*, 2829–2838.

(4) Avena, M. J.; De Pauli, C. P. *J. Colloid Interface Sci.* **1998**, *202*, 195–204.

(5) Barbier, F.; Duc, G.; Petit–Ramel, M. *Colloids Surf., A* **2000**, *166*, 153–159.

(6) Ikhsan, J.; Wells, J. D.; Johnson, B. B.; Angove, M. J. *Colloids Surf., A* **2005**, *252*, 33–41.

(7) McBride, M. B. *Environmental Chemistry of Soils*; Oxford University Press: New York, 1994.

(8) Stumm W.; Morgan J. J.; *Aquatic Chemistry*; John Wiley & Sons: New York, 1996.

(9) Bleam, W. F. *Clays Clay Miner.* **1990**, *38*, 522–526.

(10) Low, P. F. *Soil Sci. Soc. Am. J.* **1981**, *45*, 1074–1078.

(11) Klaufhold, S. *Applied Clay Sci.* **2006**, *34*, 14–21.

(12) Mortland, M. M.; Raman, K. V. *Clays Clay Miner.* **1968**, *16*, 393–398.

(13) Arroyo, L. A.; Li, H.; Teppen, B. J.; Boyd, S. A. *Clays Clay Miner.* **2005**, *53*, 511–519.

(14) Stathi, P.; Christoforidis, K. C.; Tsipis, A.; Hela, D. G.; Deligiannakis, Y. *Environ. Sci. Technol.* **2006**, *40*, 221–227.

adsorption, attributed to the surface complexation reaction with the amphoteric surface hydroxyl groups at the edge of the clay particle, and (b) a pH-independent adsorption, usually attributed to cation exchange in the interlayer space. This results from the electrostatic interaction between the ions in solution and the permanent charge.⁸ This mechanism is intimately correlated with cation exchange and therefore becomes more significant in high CEC clays, for example, smectites.^{3–6} Experimentally, the pH-independent cation uptake mechanism becomes more evident at low $\text{pH}^{3–6}$ where cations are not taken up by the amphoteric sites.

The structural permanent charge is related to the mineral structure and composition^{15,16} and is considered to remain constant for a given clay preparation. Typically, the CEC of a clay is regarded as a reference parameter which characterizes the clay. Usually, pH variation or ion sorption exerts little or zero effect to the CEC of a particular clay. Certain exceptions to this concept have been reported however.^{15–19} In this context, CEC has been shown to be altered after hard acid treatment,¹⁵ redox reactions of structural iron,¹⁷ and lithium fixations.¹⁵ For example, Li^+ fixation upon heating has a definite influence on the negative charge and CEC properties of a smectite.¹⁵ Acid treatment of clays has been reported to replace exchangeable cations with H^+ ions,¹⁵ while Al^{3+} and other cations escape from both tetrahedral and octahedral sites leaving the SiO_4 groups largely intact.¹⁸ Treatments of clays with strong acids have been argued to cause destruction of the crystalline structure of clay minerals.¹⁸ H_2SO_4 treatment of a kaolinite (CEC = 11.3 mequiv/100 g) or a montmorillonite (CEC = 153 mequiv/100 g) increased the CEC of the treated clays to 12.2 and 340 mequiv/100 g, respectively.¹⁸ In other works, acid treatment has been shown to increase the surface area and cation exchange capacity of clay minerals, eliminating also mineral impurities.^{16,17} More particularly, chemical modification of smectites, such as acid activation, iron reduction,¹⁷ fixation of cations, or combination of all three methods, has been found to affect substantially the surface area and cation exchange capacity of smectite.¹⁹

In the present work, we present the effect of a mild chemical treatment on the (a) CEC, (b) H^+ binding, (c) permanent negative charge, and (d) metal uptake properties of a Zn-containing montmorillonite.

The aim of present work was (a) to present a novel phenomenon, namely, the variation of the CEC via Zn-removal, under mild chemical treatment, (b) to study the effect of increasing CEC on the metal uptake of clays, and (c) to analyze theoretically the effect of permanent charge sites on the cation binding, including metals.

2. Materials and Methods

All solutions were prepared with analytical grade chemicals and purified water (Milli-Q, produced by Millipore Academic system) with a conductivity of demineralized water of $18.2 \mu\text{S}$. $\text{Cd}(\text{NO}_3)_2$, CH_3COONa , and CH_3COOH were purchased from Aldrich.

The clay used in this work was a high Zn-containing batch of montmorillonite clay with the code name Zenith-N, from a mining site in Milos island in Greece. This differs from the

common Zenith clays, studied in detail previously^{20–24} in its Zn content. In the present study, this less-common clay was used in order to evaluate the effects of Zn content on fundamental physicochemical properties of montmorillonite.

2.1. Chemical Treatment: Permanent Charge Sites' Alteration. For the purification of raw montmorillonite and removal of Zn, the following chemical treatment was used:²⁵ A total of 10 g of the Zenith montmorillonite was dispersed in 250 mL of Milli-Q water, and the suspension was stirred for 24 h. Then, the sample was placed in volumetric cylinder of 1 L and left to rest for 5–6 h. The suspension over the last 5 mL from the bottom of the cylinder was removed by siphoning. This contained particles with diameter $2 \mu\text{m}$. The sample was then centrifuged at 4000 rpm (1789g) for 30 min, and the obtained solid was treated with the appropriate buffer solution $\text{CH}_3\text{COOH}/\text{CH}_3\text{COONa}$ ($\text{pH} \sim 4.8$) at 70°C for 30 min. Note that, usually, the role of this buffer solution is assumed to remove carbonates absorbed by the clay mineral;²⁵ however, as we show in this work, acetate treatment can also result in efficient removal of zinc from the exchangeable sites of montmorillonite.

Three different concentrations of acetate buffer solution were used for the treatment of the samples: 0.75, 1, and 2 M (samples denoted as Zenith₁, Zenith₂, and Zenith₃, respectively) in CH_3COONa and CH_3COOH (pH always set at 4.8), while a reference sample not treated with acetate was used for comparison (denoted as Zenith). Supernatants from the acetate-treated clays were analyzed for Zn by atomic absorption spectroscopy, using an AAS700 Perkin-Elmer apparatus. Mixtures were cooled immediately, centrifuged, resuspended in 100 mL of water, and recentrifuged several times. Clay samples were then immersed into 1 M solutions of NaCl, and the procedure was repeated three times in order to prepare the Na^+ -exchanged samples. Finally, the samples were washed with distilled deionized water, transferred into dialysis tubes²⁵ to remove Cl^- ions, and dried at room temperature. Finally, in order to reveal whether the interlayer space of Zenith samples before and after chemical treatment could be expanded, ethylene glycol vapors were allowed to contact with Zenith films oriented on glass plates for 8 h at 60°C .

2.2. Structural Characterization of Montmorillonite. X-ray powder diffraction data were collected on a D8 Advance Bruker diffractometer by using $\text{Cu K}\alpha$ (40 kV, 40 mA) radiation and a secondary beam graphite monochromator. The patterns were recorded in the 2θ range from 2 to 30° , in steps of 0.02° and counting time 2 s per step. Fourier transformed infrared (FTIR) spectra were measured with a Perkin-Elmer Spectrum GX infrared spectrometer, in the region of $400\text{--}4000 \text{ cm}^{-1}$. Each spectrum was the average of 64 scans collected at 2 cm^{-1} resolution. FTIR samples were prepared in the form of KBr pellets containing $\sim 2 \text{ wt } \%$ clay.

X-ray photoelectron spectroscopy (XPS) data were collected using a Scienta R4000 spectrometer equipped with a monochromatic $\text{Al K}\alpha$ X-ray source ($h\nu = 1486.6 \text{ eV}$); the photoelectron takeoff angle was 90° , and an electron flood gun was used to compensate for sample charging; the base pressure during the measurement was $5 \times 10^{10} \text{ mbar}$. Evaporated gold films supported on mica were used as substrates. Each clay sample was dispersed in distilled–deionized water ($18.2 \text{ m}\Omega$, Milli-Q), and after stirring and sonication a small drop of the suspension was left to dry in air on the substrate. The samples were

(15) Komadel, P. *Clay Miner.* **2003**, *38*, 127–138.

(16) Prakash, K.; Raksh, V. J.; Thirumaleshwara, S. G. B. *Ind. Eng. Chem. Res.* **1995**, *34*, 1440–1448.

(17) Farve, F.; Bogdal, C.; Gavillet, S.; Stucki, J. W. *Appl. Clay Sci.* **2006**, *34*, 95–104.

(18) Bhattachariya, K. G.; Gupta, S. S. *Ind. Eng. Chem. Res.* **2007**, *46*, 3734–3742.

(19) Breen, C.; Zahoor, F. D. *J. Phys. Chem. B* **1997**, *101*, 5324–5331.

(20) Szabó, A.; Gournis, D.; Karakassides, M. A.; Petridis, D. *Chem. Mater.* **1998**, *10*, 639–645.

(21) Karakassides, M. A.; Gournis, D.; Petridis, D. *Clay Miner.* **1999**, *34*, 429–438.

(22) Gournis, D.; Mantaka, A. M.; Karakassides, M. A.; Petridis, D. *Phys. Chem. Miner.* **2001**, *28*, 285–290.

(23) Gournis, D.; Karakassides, M. A.; Boukos, N.; Bakas, T.; Petridis, D. *Carbon* **2002**, *40*, 2641–2646.

(24) Gournis, D.; Loulidi, M.; Karakassides, M. A.; Kolokytha, C.; Mitopoulou, K.; Hadjiliadis, N. *Mater. Sci. Eng., C* **2002**, *22*, 113–116.

(25) Gournis, D.; Lappas, A.; Karakassides, M. A.; Tobbens, D.; Moukarika, A. *Phys. Chem. Miner.* **2008**, *35*, 49–58.

introduced into ultrahigh vacuum as soon they were as dry. All binding energies were referenced to the silicon 2s core level of montmorillonite clay at 102.9 eV,²⁶ and the resolution was 1.4 eV. No X-ray induced sample degradation was detected. Spectral analysis included peak deconvolution employing Gaussian line shapes with the help of the WinSpec program developed at the LISE laboratory, University of Namur, Belgium.

2.3. Cation Exchange Capacity (CEC) Measurements.

CEC is a fundamental property of clay minerals, defined as a measure of the ability of clay to adsorb cations in such form that they can be readily desorbed by competing ions.²⁷ CEC is a measure of the cations which balance the permanent negative charge on clay.²⁸ In commonly used CEC measurement procedures, the negative charge of a material is balanced with selected index cations. After that, the CEC is determined by measuring the difference between the initial and the remaining content of the index cation.¹⁸ Commonly used protocols, for estimating CEC, include the ammonium acetate method,²⁹ triethanolamine buffered BaCl solution,³⁰ radioactive tracer,³¹ nephelometry,³² methylene blue,³³ Cu(II)-ethylenediamine,³⁴ and Cu(II)-triethylenetetramine.³⁵ In the present work, CEC measurements were done by using the Co(II) method.³⁶ A total of 0.5 g of the clay was suspended in 10 mL of aqueous solutions containing 0.25 M CoSO₄. The suspension was allowed to equilibrate for 3 h under stirring at pH 4.0 and then centrifuged at 4500 rpm for 30 min. This procedure was repeated twice, and then the supernatant solution was analyzed for Co with UV-vis spectrophotometry (511 nm)³⁶ as well as by atomic absorption spectroscopy. The amount of adsorbed Co(II) was calculated by the difference [Co(added) – Co(remaining in solution)]. In the present work, this will be referred as the CEC of the sample according to Co(II) method.³⁶ At pH 4.0, used herein for CEC measurements, only the permanent charge sites are available for cation uptake, since the variable charge edge-sites are all protonated. Thus, the CEC values reported herein for the clays refer exclusively to the permanent charge sites.

2.4. Surface Charge Properties of Montmorillonite.

The surface charge of montmorillonite suspensions was evaluated by potentiometric acid–base titration to quantify H⁺ uptake^{3,4,37,38} as described earlier.^{14,39,40} A total of 12.5 mg of montmorillonite was suspended in a titration cell containing 12.5 mL of Milli-Q water to yield a montmorillonite concentration of 1 g/L. The suspension was allowed to equilibrate (swelling) for 12 h under continuous stirring. Prior to titration, the sample solution was purged with N₂ for 30 min and divided into two equal portions, one for acidimetric titration and one for alkalimetric titration.³⁷ The acidimetric titration was done with 12.5 mM HNO₃ in the pH range 3.00–9.25, and the alkalimetric titration was done with 12.5 mM NaOH with pH range 9.25–10.50. In all titrations, a Metrohm 794 Basic Titrino buret was used, and the pH was measured with a Metrohm Pt-glass electrode (type 6.0239.100). A new amount of acid or base was added when

the electrode drift was lower than 0.05 pH units/min. Typically, each titration was accomplished within 2–2.5 h.

2.5. Metal Sorption. Cd²⁺ sorption experiments were performed at 24 °C, as described earlier^{14,39,40} for clay suspensions at concentrations of 1 g/L in polypropylene tubes. Cd²⁺ adsorption was investigated in batch experiments. Cd²⁺ was chosen as a representative heavy metal, studied in environmental physical chemistry experiments with clays and oxides. Sorption pH-edge experiments were performed to measure the effect of pH on the metal uptake as follows: zenith clay was suspended in polypropylene tubes containing a buffer system of 10 mM MES (*N*-morpholino-ethanesulfonic acid); 10 mM HEPES (4-(2-hydroxyethyl)piperazine-1-ethanesulfonic) was used for all of the samples. This system presented a significant buffer capacity at the pH range 5.0–8.5 with an average deviation from the adjusted pH value of <5%. Screening experiments indicated that under the conditions of our experiments the buffer molecules caused no interference on the adsorption phenomena. The pH was adjusted with small volumes of NaOH (0.1 N) or HNO₃ (0.05 N), and each suspension was allowed to equilibrate (swelling) for 12 h under continuous stirring. In the following, a suitable volume of Cd(NO₃)₂ stock solution was added to yield a Cd²⁺ concentration of 4.5 μM. The pH of the suspension was readjusted, if necessary, by using small amounts of HNO₃ or NaOH. The sample was allowed to equilibrate at room temperature for 2 h under stirring. Screening experiments showed that Cd uptake equilibrium was attained within 40 min (data not shown). The pH of each suspension was continuously monitored and readjusted if necessary. Typically, in the present experiment, pH variations did not exceed ±0.1 pH units. Finally, the sample was centrifuged and the supernatant solution was analyzed for Cd²⁺.

Analytical Measurements. The concentration of cadmium in the aqueous phase was determined by anodic stripping voltammetry using a Trace Master-MD150 polarograph by Radiometer Analytica. The working electrode was a hanging mercury drop electrode (Hg drop diameter 0.4 mm), generated by a 70 μm capillary. The reference electrode was an Ag/AgCl electrode with a double liquid junction. The counter electrode was a Pt electrode. Initially, before the stripping step, pure N₂ gas (99.999% purity) was bubbled through the measuring solution to remove any trace O₂. During this step, the solution was under continuous stirring at 525 rpm. Square wave (SW) measurements were performed in the anodic direction; that is, square wave anodic stripping voltammetry was used⁴⁰ to quantify Cd²⁺. Typically, under our experimental conditions, 10^{−6} M Cd(NO₃)₂ at pH 5.4 in 0.01 M KNO₃ resulted in a current of I_p = 0.980 μA at E_p = −460 mV.

Zn concentration in the clay and the supernatant was measured by atomic absorption spectrophotometry (AAS) using a Perkin-Elmer Analyst A700 Flame-Graphite Furnace AAS instrument. For measuring Zn concentration in the clay, 10 mg of clay material was digested for 24 h in 10 mL (65%) of HNO₃. Then, the sample was analyzed for Zn content by AAS. Background Zn content in HNO₃ (<10 ppb) was negligible.

2.6. Theoretical Analysis: Surface Complexation Modeling.

The results of all potentiometric titration and Cd²⁺ sorption experiments were modeled with a surface complexation model⁴¹ (SCM) by assuming that adsorption involves both a coordination reaction at specific surface sites and an electrostatic interaction between adsorbing ions and the charged surface. Previously, SCMs have been used extensively to describe the adsorption of various ionic species on charged surfaces⁴¹ including clays.^{39,40} Following standard notation, in our modeling, we have assumed two different populations of surface reactive sites (≡SOH) representing amphoteric aluminol and silanol groups on the mineral edge. Proton binding at these sites was modeled assuming

(26) Barr, T. L. *Appl. Surf. Sci.* **1983**, *15*, 1–35.

(27) Czimmerova, A.; Bujdak, J.; Dohrmann, R. *Appl. Clay Sci.* **2006**, *34*, 2–13.

(28) Tournassat, C.; Greneche, J. M.; Tisserand, D.; Charlet, L. *J. Colloid Interface Sci.* **2004**, *273*, 224–233.

(29) Mermut, A. R.; Lagaly, G. *Clays Clay Miner.* **2001**, *49*, 393–399.

(30) Bascomb, C. L. *J. Sci. Food Agric.* **1964**, *15*, 821–823.

(31) Bache, B. W. *J. Sci. Food Agric.* **1971**, *27*, 273–280.

(32) Adams, J. M.; Evans, S. *Clays Clay Miner.* **1979**, *27*, 137–139.

(33) Hang, P. T.; Brindley, G. W. *Clays Clay Miner.* **1970**, *10*, 203–212.

(34) Bergaya, F.; Vayer, M. *Applied Clay Sci.* **1997**, *12*, 275–280.

(35) Meier, L. P.; Kahr, G. *Clays Clay Miner.* **1999**, *47*, 386–388.

(36) Rhodes, C. N.; Brown, D. R. *Clay Miner.* **1994**, *29*, 799–801.

(37) Schulthess, C.; Sparks, D. L. *Soil Sci. Soc. Am J.* **1986**, *50*, 1406–1411.

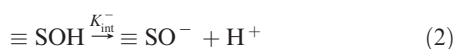
(38) Wanner, H.; Albinsson, Y.; Karnald, O.; Wieland, E.; Wersin, P.; Charlet, L. *Radiochim. Acta* **1994**, *66*(67), 157–162.

(39) Giannakopoulos, E.; Stathi, P.; Dimos, K.; Gournis, D.; Sanakis, Y.; Deligiannakis, Y. *Langmuir* **2006**, *22*, 6863–6873.

(40) Stathi, P.; Litina, K.; Gournis, D.; Giannopoulos, T. S.; Deligiannakis, Y. *J. Colloid Interface Sci.* **2007**, *316*, 298–309.

(41) Dzombak, D. A.; Morel, F. M. M. *Surface Complexation Modeling*; John Wiley & Sons: New York, 1990.

the following reactions:



The equilibrium constants of H^+ reacting with the surface sites were expressed in the form

$$K_{\text{int}}^+ = \frac{[\equiv \text{SOH}_2^+]}{[\equiv \text{SOH}][\text{H}^+]} e^{[F\Psi_0/RT]} \quad (3)$$

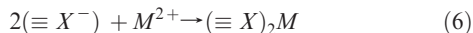
$$K_{\text{int}}^- = \frac{[\equiv \text{SO}^-][\text{H}^+]}{[\equiv \text{SOH}]} e^{[-F\Psi_0/RT]} \quad (4)$$

where Ψ_0 is the electrostatic surface potential, F is the Faraday constant, R is the gas constant, and T is the absolute temperature. The values of the intrinsic equilibrium constants K_{int}^+ and K_{int}^- were determined by fitting the experimental data.³

The equilibrium constant of metal reacting with clay surface sites was expressed in the form

$$K_{(M+2)} = \frac{[\equiv \text{XOM}^+][\text{H}^+]}{[\equiv \text{XOH}](M+2)} e^{[-F\Psi_0/RT]} \quad (5)$$

Permanent charge, cation exchange sites ($\equiv \text{X}^-$) were also taken into account⁴ by assuming reaction 6.



This modeling approach was adapted from previous successful applications for adsorption of metals and organics on kaolinite⁴² and montmorillonite^{3,4,6,40,43} and recently for a synthetic montmorillonite Laponite.³⁹

We underline that, in the present case, inclusion of permanent charge, cation exchange sites ($\equiv \text{X}^-$) had a decisive effect on the adsorption data, becoming particularly evident at acidic pH. The conceptual model is as follows: in montmorillonites, binding of metals at the $\equiv \text{X}^-$ sites is expected to be pH-independent.^{3,4,39,40,43} Therefore, in a pH-edge experiment, binding of the metal at the $\equiv \text{X}^-$ sites will be manifested as a pH-independent upshift of the metal binding curve at low pH. This was originally observed experimentally and analyzed by Bayens and Bradbury⁴³ and verified by other groups.^{3,4,39,40,43} In the present work, for simplicity, we did not consider heterogeneity in the binding sites.⁴³ The surface and solution reactions are summarized in Table 4. All calculations were performed using the FITEQL program.⁴⁴

Effect of Permanent Charge on the Point of Zero Charge. In our montmorillonite clay, the $\equiv \text{X}^-$ site concentration was approximated^{3,4,6} by the CEC value. Kraepiel et al.³ have pointed out that the $\equiv \text{X}^-$ sites can create a charge density which may influence the surface proton binding constants, that is, via the Boltzman term. The permanent charge density can be estimated from the following equation

$$\sigma_0 = F[\text{X}^-]/s \quad (7)$$

for a specific area (BET) $s = 300 \text{ m}^2/100 \text{ g}$ measured for our clay.

Including this σ_0 value in the calculation of the point of zero charge, by the formula of Kraepiel et al.,³

$$\text{pH}_{\text{pzc}} = \frac{1}{2}(\text{p}K_{\text{int}}^+ + \text{p}K_{\text{int}}^-) - \frac{1}{2.3} \left(\frac{F\Psi_0}{RT} \right) \quad (8)$$

where

$$\frac{F\Psi_0}{RT} = 2 \text{arcsinh} \left(\frac{\sigma_0}{0.1174\text{I}^{1/2}} \right) \quad (9)$$

and I is the ionic strength. As an example, for a CEC 76.4 mequiv/100 g, typical for SWy-2 montmorillonite,³ the permanent charge density is estimated as $\sigma_0 = 18.3 \times 10^{-3} \text{ C/m}^2$. By using eqs 8 and 9, this charge density is predicted to cause a shift of the pH_{pzc} from 8.35 to 8.23, that is, 0.12 pH units. This is a rather small, though nonzero, shift resolvable experimentally.³ For higher CEC values, this effect will be more prominent, as we show in the present case.

3. Results

3.1. Structural Characterization of Montmorillonite Samples. X-ray diffraction (XRD) measurements provide a powerful tool to understand the changes in the interior of the clay microenvironment, since the interlayer distance can be estimated by measuring the d_{001} spacing. XRD patterns for Zenith, Zenith₁, Zenith₂, and Zenith₃ are shown in Figure 1. The basal spacing (d_{001}) in all samples is almost the same, indicating that the interlayer separation was not affected by the chemical treatment with acetate solutions. In addition, the 060 reflection of the samples (Figure 1, inset) can not only provide supporting information for the type of the clay but also help to identify if structural changes occurred in the clay samples before and after the chemical treatment.⁴⁶ The 060 reflection of the untreated Zenith is at $2\theta = 61.9^\circ$ with a d -spacing of 1.50 Å, which corresponds to a typical dioctahedral clay mineral, such as montmorillonite. Similar 060 values are also observed in the case of Zenith₁ (61.8°), Zenith₂ (61.8°), and Zenith₃ (61.9°), indicating that the chemical treatment with buffer acetate solutions does not cause any drastic structural modification of the clay lattice.

Finally, in order to reveal whether the interlayer space of Zenith samples -before and after chemical treatment- could expand or not, ethylene glycol vapors were allowed to contact with Zenith films oriented on glass plates. The ethylene-glycol-treated clays usually contain a single or double layer of ethylene glycol molecules between consecutive silicate layers giving d_{001} spacings of 13.5 and 16.8 Å, respectively.⁴⁶ In our samples, the basal spacing in all samples, before and after chemical treatment with acetate solutions (Figure 1, inset B), is almost the same and equal to $d_{001} \sim 16.7$ Å, indicating the formation of a double-layer arrangement of the ethylene glycol molecules in the interlayer. Moreover, this experiment provides evidence that the expandability of the clay is not affected by the acetate treatment.

The FTIR spectra for Zenith, Zenith₁, Zenith₂, and Zenith₃ (Figure 2) present the characteristic bands of clay mineral, without significant changes, indicating that the aluminosilicate mineral remained unaffected upon chemical treatment. Specifically, the peak 3636 cm^{-1} is attributed to clay lattice $-\text{OH}$ stretching vibrations, while at 3463 and 1632 cm^{-1} appears the adsorbed H_2O deformation. Bands at 1037 , 523 , and 465 cm^{-1} originate from the $\text{Si}-\text{O}$ and $\text{Si}-\text{O}-\text{Si}$ vibrations of the clay lattice. Finally, the absence of peaks due to $-\text{CH}_2-$ and $-\text{CH}_3$ vibrations, at 2800 – 2950 cm^{-1} as well as at 1385 and 1455 cm^{-1} (present in the spectrum of Zenith, Figure 2a), reveals that organic contaminants were effectively eliminated during the purification process. More particularly, the FTIR data show the absence of acetate in the treated clays.

(42) Benyahya, L.; Garnier, J. M. *Environ. Sci. Technol.* **1999**, *33*, 1398–1407.

(43) Baeyens, B.; Bradbury, M. H. J. *Contam. Hydrol.* **1997**, *27*, 199–222.

(44) Herbelin, A.; Westall, J. *FITEQL: A computer program for determination of chemical equilibrium constant from experimental data*, version 4.0, report 99-01; Department of Chemistry, Oregon State University: Corvallis, OR, 1999.

(45) Hufner S. *Photoelectron Spectroscopy Principles and Applications*; Springer Verlag: Berlin, 2003.

(46) Gournis, D.; Mantaka-Marketou, A. E.; Karakassides, M. A.; Petridis, D. *Phys. Chem. Miner.* **2000**, *27*, 514–521.

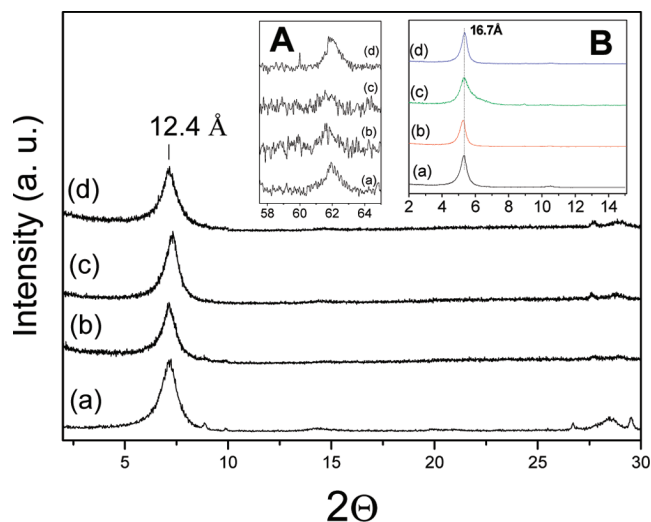


Figure 1. XRD patterns of (a) Zenith, (b) Zenith₁, (c) Zenith₂, and (d) Zenith₃. Inset A: 060 reflection region. Inset B: XRD patterns of the same Zenith samples after contact with ethylene glycol vapors.

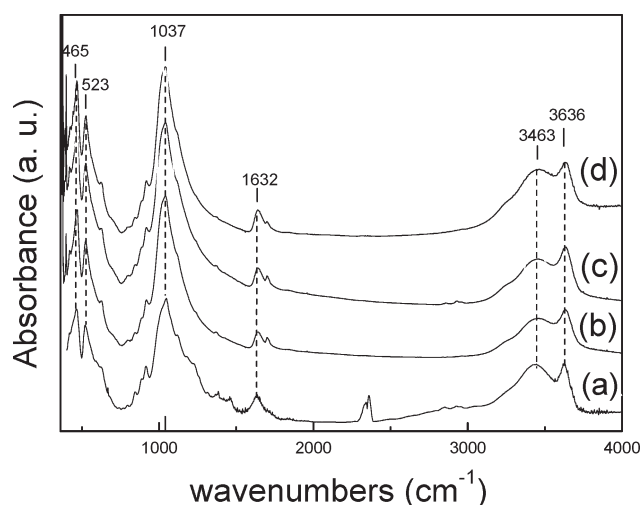


Figure 2. FTIR spectra of (a) Zenith, (b) Zenith₁, (c) Zenith₂, and (d) Zenith₃.

Overall the XRD and FTIR data indicate that the structural units, expandability, and lamellar structure are not modified by the treatments applied to Zenith montmorillonite samples. However, as we show in the following, other physicochemical properties were severely influenced.

XPS is a direct method for identifying the surface elemental composition of a material (quantitative analysis); therefore, this method was used to investigate the metal content within the clay stack and thereby confirm Zn removal. Figure 3 shows a representative XP scan of the low binding energy region (from 0 to 180 eV) collected from pristine Zenith. As labeled in the figure, characteristic photoelectron and Auger peaks of O, Na, Si, Al, Fe, and Mg are clearly distinguishable. Detailed scans of the carbon (C1s) and calcium (Ca2p) regions (not shown here) reveal the presence of these elements. The small carbon peak is mainly due to contaminant carbon species always present on the outer surface of air exposed materials, but it is also caused by soil organic matter present in natural clay minerals. Detailed scans of the zinc 2p region are displayed in Figure 4 for Zenith and Zenith₃. Four low binding energy peaks, attributed to Auger excitations of the oxygen atoms (labeled O KLL in the figure and marked by dotted lines), are present for both pristine Zenith and

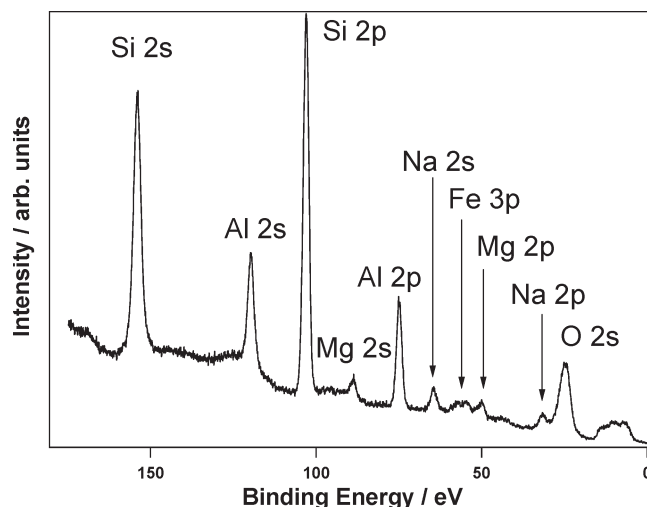


Figure 3. XP spectrum of pristine Zenith.

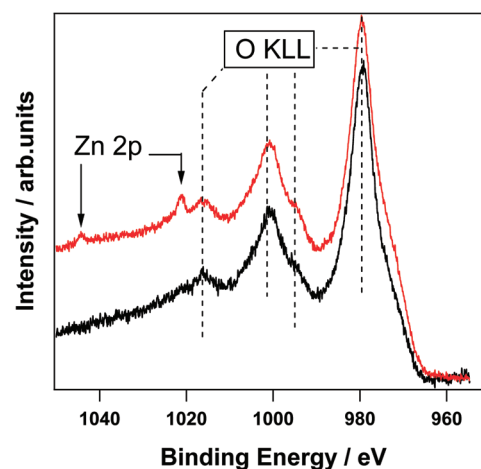


Figure 4. XP spectra of the oxygen KLL Auger and zinc 2p photoelectron peaks of Zenith (top) and Zenith₃ (bottom).

clay treated with acetate buffer solution (Zenith₃). On the high binding energy side, one can clearly see, in the pristine Zenith sample, the occurrence of two components around 1022 and 1044 eV attributed to the zinc 2p_{3/2} and 2p_{1/2}, respectively. These peaks are absent (or barely visible) in the XP curve of the Zenith₃ sample, revealing that zinc was efficiently eliminated from the clay during the chemical treatment. Unfortunately, the intensities of the Zn2p core lines and of the Zn L₃M₄₅M₄₅ Auger peak (not shown) of pristine clay Zenith were too small to allow a reliable determination of the Zn oxidation state.

XPS provides not only qualitative but also quantitative information about the composition of the samples; the peak areas of all elements, normalized for the relative cross sections at the photon energy of 1486.6 eV used in the experiments and analyzer transmission, are proportional to the amount of corresponding atoms within the sampling depth. If we calculate the Zn content assuming that Zn sits at the *surface* of our samples, we obtain a Zn stoichiometry which is clearly much lower than the Zn content of the clay, for example, as determined by atomic absorption spectroscopy, listed in Table 1. However, if we take into account that Zn is situated in the *interlamellar space* and thus the Zn2p are attenuated by the passage through the clay platelet,⁴⁵ we estimate a Zn stoichiometry of 0.28 (±0.03). This is in agreement with the estimate of Zn by the AAS analytical data, listed in Table 1. Importantly, the combination of AAS and XPS analysis provides

evidence that in the pristine clay Zn is localized at the interlayer space of the clay. The chemical composition of pristine clay Zenith before and after chemical treatment with 2 M acetate solution is given in Table 1 (all the values normalized to Si, assuming that Si is 8).

3.2. CEC and Zn Measurements. The CEC and the Zn content of the montmorillonite samples treated with different concentrations of acetate buffer are shown in Table 1.

From Table 1, we observe that the CEC of montmorillonite increased for increasing concentrations of acetate. The trend is verified for other acetate treatments such as 0.7, 1.25, 1.5 M acetate, giving CEC values 58, 136, and 167 mequiv/100 g and Zn contents 90, 56, and 34 mmol/100 g, respectively. This shows that the acetate treatment affects the permanent charge sites. Analogous observation was made by Bhattacharyya and Gupta¹⁸ who reported that the CEC value for their kaolinite and montmorillonite clay was 11.3 and 153 mequiv/100 g, respectively, and

Table 1. CEC, Zn Content, and Composition of Zenith Montmorillonite Treated with Different Concentrations of Acetate

sample	CEC (mequiv/100 g)	acetate concentration (M)	Zn content	
			(mmol/100 g) ^a	(mequiv/100 g) ^a
Zenith	38.4	no acetate	98	196
Zenith ₁	58.5	0.75	90	180
Zenith ₂	77.0	1.00	77	154
Zenith ₃	180.0	2.00	13	26

clay composition derived from XPS^b

Zenith

Si, 8.0; Al, 3.2(±0.1); Mg, 0.60(±0.02); Ca, 0.22(±0.01); Fe, 0.32(±0.01); Zn, 0.28(±0.03); O, 23.2(±0.7)

Zenith₃

Si, 8.0; Al, 3.1(±0.1); Mg, 0.62(±0.02); Ca, 0.20(±0.01); Fe, 0.30(±0.01); Zn, 0.0; O, 23.5(±0.7)

^a Estimated assuming all Zn to be Zn²⁺ ions. ^b All the values have been normalized to Si, assuming Si = 8.

upon acid treatment with H₂SO₄ the CEC values were increased to 12.2 and 340 mequiv/100 g, respectively.¹⁸ The harsh acid treatment in ref 18 resulted in severe damage of the lattice structure.¹⁸ This probably is the origin of the unprecedented 4-fold increase in the CEC of montmorillonite found in ref 18. In contrast, in the present case, FTIR, XRD, and XPR data show that acetate treatment leaves the clay structure intact. In the following, the structural significance and origin of the observed CEC modification was further probed by H⁺-binding and metal binding experiments.

3.3. Charge Properties of Montmorillonite Samples.

Figure 5A1–D1 shows the potentiometric titration data for the montmorillonite sample. The solid lines in Figure 5A1–D1 represent the theoretical fit to the experimental data obtained by assuming the reactions listed in Table 4. In panels A2–D2, we display the ensuing theoretical speciation scheme, derived from the fit. According to this, at pH 3–5.5, we observe a rapid loss of protons from the surface ≡SOH₂⁺ groups, attaining a plateau at pH 5.5–8, and then the rapid loss of protons at pH > 9 is due to deprotonation of surface groups resulting in the formation of ≡SO[−] surface species. Noticeably, in all samples, the derived protonation constants were comparable $K_{\text{int}}^+ = 8.9 \pm 0.1$ and $K_{\text{int}}^- = -9.1 \pm 0.1$, listed in Table 2. This shows that acetate treatment despite its effect on the CEC did not influence the protonation properties of amphoteric ≡SOH groups.

Influence on the pH_{PZC} . According to Kraepiel et al.,³ the observed considerable changes of the CEC sites should be reflected in changes in the permanent charge. This in turn is expected to have an impact on the point of zero charge of the clay. This can be estimated by the method of Kraepiel et al.³ (see Table 2). Acetate treatment exerts a nonzero effect on the point of zero charge of the clay. From Table 2, we see that treatment with 2 M acetate (Zenith₃) decreases the pH_{PZC} by 0.21 pH units relative to Zenith.

3.4. Correlation CEC versus [Zn Content] on Zenith Clay. Figure 6A shows a correlation plot of the Zn content of the clay measured for Zenith montmorillonite versus acetate concentration used for clay treatment. According to Figure 6A, the Zn content decreased for increasing acetate concentration. The Zn content of the clay before acetate treatment was

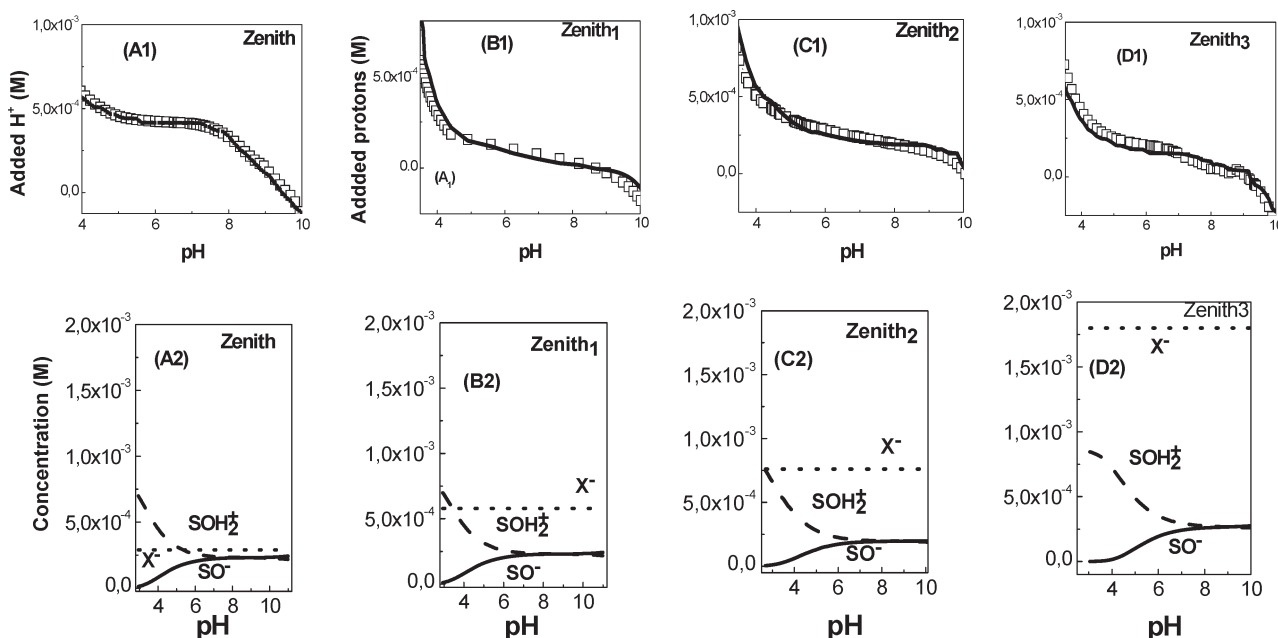


Figure 5. Surface charge properties for Zenith clay. (A1–D1) Potentiometric acid–base titration (□) experimental data and (solid line) theoretical model based on FITEQL by using the parameters listed in Table 4. (A2–D2) Theoretical speciation of surface species.

103 mmol/100 g and diminished to 13 mmol/100 g after treatment with 2 M acetate at pH 4.8.

This indicates that treatment with acetate (at pH 4.8) removes Zn from the clay. Control measurements, for Zn release at pH 4.8 adjusted with HNO_3 with no acetate present, showed that Zn release from the clay was less than 2% (data not shown). Overall, the present data provide evidence that pH is not the factor responsible for Zn removal. Acetate acts as a specific agent enhancing Zn removal. Although the stability constant for $[\text{Zn acetate}]$ is relatively low ($\log K = 1.6$),⁸ the Zn removal is achieved efficiently, however, only at very high acetate concentrations (up to 2 M). On the other hand, the requirement of high acetate concentrations provides evidence that in this clay Zn should be bound relatively strongly in the clay.

Figure 6B shows the Zn content on Zenith montmorillonite versus CEC of the clay and documents a linear anticorrelation between Zn content and CEC, with a slope of Zn versus CEC of nearly -2 . This slope indicates that, for each Zn removed, 2 cation exchange sites become available in the clay. Based on this quantitative relationship, we suggest that the removed Zn species are Zn^{2+} ions.

Overall the present data demonstrate that a mild chemical treatment with acetate specifically removes Zn^{2+} ions from

the clay. This in turn is linearly anticorrelated with the permanent charge and the CEC of the clay. Importantly, the XRD data (Figure 1), the FTIR data (Figure 2), and the XPS data (Figures 3 and 4) show that the lamellar structure of clay and the main structural units of the clay remain unaltered. The H uptake data show that the pK values and the concentration of the variable charge sites are not modified by the acetate treatment.

3.5. Cd^{2+} Adsorption. Figure 7 shows Cd^{2+} uptake by Zenith clays, treated with different concentrations of acetate. In Figure 7A, we notice that (a) in all samples, Cd^{2+} uptake capacity was increased with increasing pH. This is a well documented phenomenon for the adsorption of metal cations on clays^{40,43} and will be further discussed in the following. (b) More importantly, in acetate-treated clay samples, we observe a progressive global upshift of Cd^{2+} adsorption at all pH values, relative to Zenith. For example, at pH = 4.0, Cd^{2+} uptake by Zenith₂ was 0.75 mmol/kg versus 0.27 mmol/kg for Zenith₁.

In Figure 7, we observe an enhancement of Cd^{2+} uptake at pH = 4.0 by 2.0 mmol/kg for Zenith₃ when compared with Zenith₁. At pH = 8.0, Cd^{2+} uptake was increased from 2.34 mmol/kg (for Zenith₁) to 2.97 mmol/kg (Zenith₂) and 3.72 mmol/kg (Zenith₃). For comparison, in Table 3, we list the amount of Cd^{2+} adsorbed per unit mass on different samples of Zenith montmorillonite at pH 4.0 and 8.0.

The data in Figure 7 and Table 3 show that modification of the clay by acetate may provide a protocol for engineering of the Cd uptake capacity of the clay in a controllable manner.

3.6. Probing the Metal Uptake Mechanism. Literature data for metal uptake by montmorillonites showed that the pH-independent part of adsorption can be attributed to metal binding at $\equiv\text{X}^-$ sites.^{40,43} The present data allow for a more detailed evaluation of this mechanism. The theoretical analysis (Figure 7A, open symbols) and the ensuing speciation (Figure 8)

Table 2. Protonation Constants and Charge Properties of Zenith Samples^a

sample	$\log K_{\text{int}}^+$	$\log K_{\text{int}}^-$	permanent charge (σ_0), C/m ²	pH _{pzc} estimated using the method of Kraepiel et al. ³
Zenith	8.9	−9.1	−9.12	8.90
Zenith ₁	8.9	−9.1	−14.01	8.84
Zenith ₂	8.9	−9.1	−18.44	8.82
Zenith ₃	8.9	−9.1	−43.12	8.69

^a Errors: $\log K \pm 0.1$; $\text{pH}_{\text{pzc}} = 0.5(\log K_{\text{int}}^+ + \log K_{\text{int}}^-) = 9.0$.

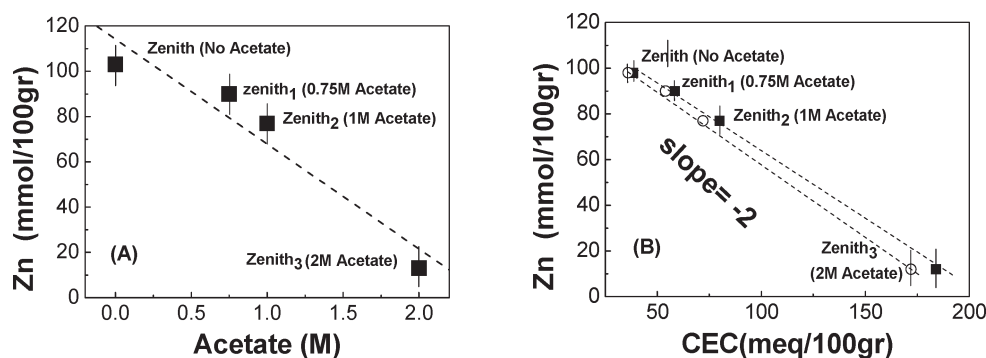


Figure 6. (A) Correlation of Zn content on Zenith montmorillonite versus acetate concentration used for clay treatment at pH = 4.8. (B) Correlation plot for Zn content on Zenith montmorillonite versus CEC of the clay; (■) CEC calculated based on Co^{2+} estimate by UV-vis and (○) CEC calculated based on Co^{2+} estimate by AAS.

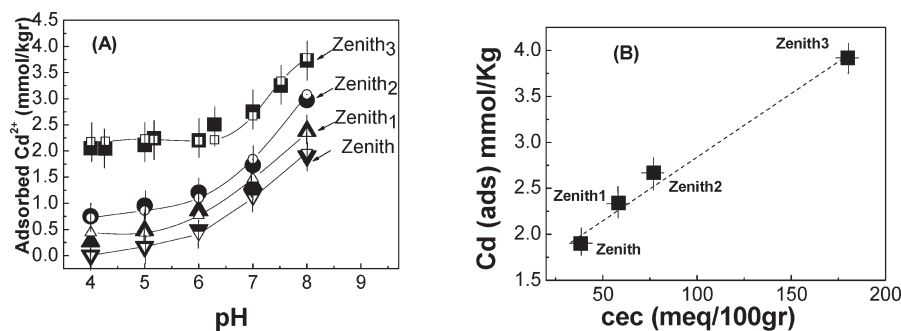


Figure 7. (A) Adsorption of Cd^{2+} on Zenith montmorillonite: (▼/▽) Zenith, (▲/△) Zenith₁, (○/●) Zenith₂, and (□/■) Zenith₃. Initial Cd^{2+} concentration = $4.5 \mu\text{M/g}$ clay. Solid symbols represent experimental data, and open symbols represent theoretical predictions calculated by FITEQL using the parameters listed in Table 4. (B) Correlation plot of maximum Cd adsorption, at pH 8.0, versus CEC of the clay.

describe in a consistent manner the observed metal uptake mechanism by the clay materials. The theoretical reactions and stability constants used in the calculations are listed in Table 4. According to the speciation scheme (Figure 8), the pH-independent part of Cd^{2+} uptake at pH 4–5.5 is attributed to adsorption on permanent negative charge sites ($\equiv X^-$), described by reaction 6. The pH-dependent part of Cd^{2+} uptake is attributed to surface complexation reaction with amphoteric surface $\equiv\text{SO}^-$ groups at the edge of the clay particle. According to Figure 8, this mechanism is enhanced at pH 6–8, where the Cd^{2+} ions are preferentially bound by the $\equiv\text{SO}^-$ sites.

According to Figure 8, the permanent charge sites ($\equiv X^-$) are responsible for metal uptake at low pH. The derived $\log K(X_2M) = 2.44$, listed in Table 4, is comparable for all Zenith samples. Moreover, this $\log K(X_2M)$ value is comparable with previous estimates for $\log K(X_2M)$ reported for Cd^{2+} uptake by SWy-montmorillonite.⁴⁰ This implies that the observed increase on the concentration of the X_2M species is not due to alteration of the molecular properties of the ($\equiv X^-$) sites. The modeling presented in Figure 8 shows that the observed increase in concentration of the X_2M species is due solely to the increase of the concentration of ($\equiv X^-$) sites.

The amphoteric sites ($\equiv\text{SO}^-$) remain unaffected by the acetate treatment, both concerning their concentration as well as their stability constants for Cd^{2+} complexation. Thus, according to the theoretical analysis, the progressive increase of ($\equiv X^-$) sites makes the $X_2\text{Cd}$ species progressively more abundant. It is characteristic that in Zenith₃ $X_2\text{Cd}$ species supersede SOCd species, even at alkaline pH (see rightmost panel in Figure 8).

In summary, taking into account the CEC versus Zn data as well as the Cd^{2+} speciation scheme, we suggest the following mechanism: the enhanced Cd^{2+} uptake by acetate-treated montmorillonite at low pH < 5 can be attributed to the enhanced formation of the $X_2\text{Cd}$ species which is due to the increased concentration of the ($\equiv X^-$) sites, caused by removal of Zn by

Table 3. Amounts (mmol/kg) of Cd^{2+} Adsorbed by Zenith Clays ($\text{Cd}_{\text{initial}} = 4.5 \text{ mmol/kg}$)^a

sample	pH 4.0 (mmol/kg)	pH 8.0 (mmol/kg)
Zenith	0.12	1.90
Zenith ₁	0.27	2.34
Zenith ₂	0.75	2.67
Zenith ₃	2.05	3.92

^a Error: $\pm 0.05 \text{ mmol/kg}$.

acetate. The stability constant of the $X_2\text{Cd}$ species is not affected. The amphoteric sites ($\equiv\text{SOH}$) remain unaffected by the acetate treatment, with regard to their concentration, their stability constants for H^+ binding, as well as their Cd^{2+} complexation.

4. Discussion

The present data reveal that the permanent charge, CEC, and Cd^{2+} uptake of Zenith clays can be largely influenced by a mild chemical treatment with acetate buffer solution. The lamellar structure of the clay remains unaffected. By controlling the concentration of acetate, Zn^{2+} can be removed in a precise and controllable way. This in turn allowed the production of clay with controllable permanent charge and CEC. The data for Cd^{2+} uptake by the modified clays show that permanent charge sites ($\equiv X^-$) can become the determinant metal adsorbing centers.

On the Role of Zn. In our work, Zn^{2+} ions are most likely the species modulating the properties of the clay. The requirement for relatively high acetate concentration provides evidence that Zn^{2+} is held relatively tightly by the clay structure. With the data at hand, however, we cannot further probe the details of the Zn location and coordination. Despite that, in light of the unusual findings in the present work, we attempt to discuss some working models taking into account previous data and ideas. Previously,

Table 4. Equilibrium Equations and Optimized Constants of Reactions

reaction	$\log K^a$	ref
Solution Reactions		
dissociation of water $\text{H}_2\text{O} \leftrightarrow \text{H}^+ + \text{OH}^-$	14.0	
hydrolysis of metals $\text{Cd}^{2+} \leftrightarrow \text{Cd}(\text{OH})^+ + \text{H}^+$	10.0	53
Surface Reactions		
protonation of clay $\text{SOH} \leftrightarrow \text{SO}^- + \text{H}^+$	−9.1	this work, ³⁴
$\text{SOH} + \text{H}^+ \leftrightarrow \text{SOH}_2^+$	8.9	this work, ³⁴
sorption of metals onto clay $2(\equiv X^-) + \text{Cd}^{2+} \leftrightarrow [\equiv X_2\text{Cd}]$	2.44	this work, ³⁴
$\text{SO}^- + \text{Cd}^{2+} \leftrightarrow \text{SOCd}^+$	3.15	this work, ³⁴
$\text{SO}^- + \text{Cd}(\text{OH})^+ \leftrightarrow \text{SOCd}(\text{OH})$	2.13	this work, ³⁴

^a Error ± 0.1 .

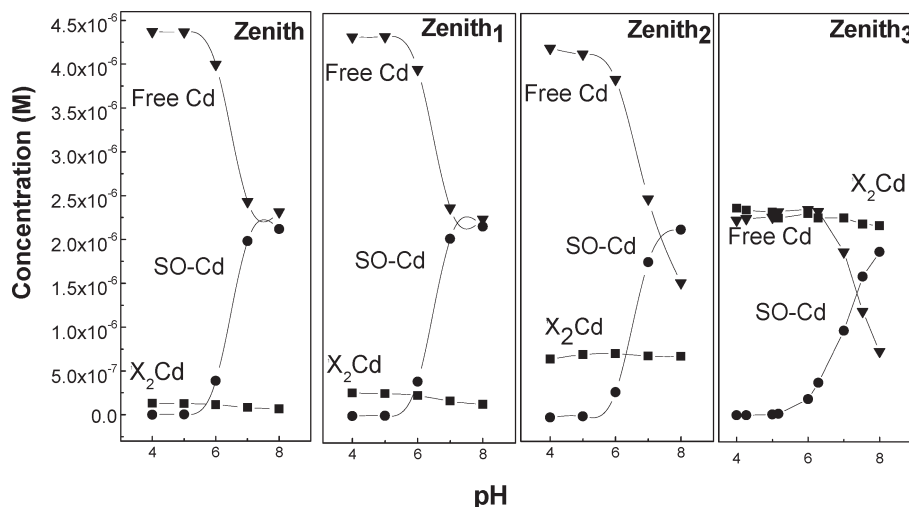


Figure 8. Theoretical speciation analysis for Cd^{2+} adsorption by the modified montmorillonites.

an EXAFS study⁴⁷ of Zn interaction with clays showed that the interaction of Zn^{2+} with smectites⁴⁷ involves formation of inner- and outer-sphere complexes. That work probed the interaction Zn with clay for both short (days) and long periods (months).⁴⁷ The mechanism of specific adsorption at alkaline pH was suggested to involve formation of $\text{Zn}(\text{OH})^+$.⁴⁷ The long-term process, that decreased the activity and extractability of Zn retained by montmorillonites,⁴⁷ was suggested to be important in the availability of Zn added to soils and the remediation of soils contaminated with Zn.⁴⁷ Brown⁴⁸ found that increasing amounts of strongly bound Zn could be removed by using salt solutions of increasing acidity. Similarly to our finding here, this strongly bound Zn had been shown to lower the exchange capacity of clay mineral.⁴² Tiller and Hodgson⁴⁹ assumed that nonextractable Zn (using 2.5% acetate) is associated with the filling of lattice vacancies in the silicate layer. However, XRD has failed to reveal any changes in the structure of silicate. However, Reddy and Perkins⁵⁰ postulated that the Zn^{2+} enters the interlayer spaces and gets trapped as the crystal contracts upon drying. Elgabaly and Jenny⁵¹ showed that part of Zn^{2+} sorbed on montmorillonite could not be exchanged by ammonium acetate at 9 mM concentrations. This strongly bound Zn^{2+} was considered to have entered the crystal lattice, and in a later work Elgabaly⁵² found that fixation of Zn^{2+} by many minerals was entirely due the lattice penetration. Overall, the cited works provided evidence that Zn^{2+} may penetrate in the structure

of clay in an irreversible manner. Our data suggest that in our montmorillonite Zn^{2+} is localized close to the interlamellar space.

5. Conclusion

Fundamental physicochemical properties such as CEC, permanent charge, pH_{pzc} , and metal uptake of a Zn-containing montmorillonite can be modified in a controllable manner, based on a chemical treatment using acetate. A linear relationship between Zn content and CEC, with a slope of $\Delta[\text{Zn}]/\Delta[\text{CEC}] = -2$, is revealed, which shows that, for every Zn removed, two cation exchange sites become available in the clay. Based on this quantitative relationship, we suggest that the removed Zn species are Zn^{2+} ions. Removal of zinc is supported by the surface elemental analysis derived from the XPS spectra. Importantly, the XRD and FTIR data show that the lamellar structure of clay and the main structural units of the clay are retained during this treatment. The H uptake data show that the pK values and the concentration of the variable charge sites are not modified by the acetate treatment. Overall, these data demonstrate that a mild chemical treatment with acetate specifically removes Zn from the clay structure and that this in turn linearly anticorrelates with the permanent charge and the CEC of the clay, thus providing additional ($\equiv\text{X}^-$) sites which can become the determinant metal adsorbing centers.

Acknowledgment. A.E. gratefully acknowledges the Academy of Athens for a Ph.D. fellowship. The authors acknowledge the use of the XRD unit of the Laboratory Network, UOI.

(53) Baes, C. F.; Mesmer, R. E. *The Hydrolysis of Cations*; R.E. Krieger Publishing Co.: Malandar, 1986.

(47) Lee, S.; Anderson, P. R.; Bunker, G. B.; Karanfil, C. *Environ. Sci. Technol.* **2004**, *38*, 5426–5432.

(48) Brown, A. L. *Soil Sci.* **1950**, *69*, 349–358.

(49) Tiller, K. G.; Hodgson, J. F. *Clays Clay Miner.* **1962**, *9*, 393–403.

(50) Reddy, M. R.; Perkins, H. F. *Soil Sci. Soc. Am. J.* **1974**, *38*, 229–231.

(51) Elgabaly, M. M.; Jenny, H. J. *Phys. Chem.* **1943**, *47*, 399–408.

(52) Elgabaly, M. M. *Soil Sci.* **1950**, *69*, 167–174.